Compatibility in Polymer/Plasticizer Blend System: Thermal, X-ray, and Dynamic Mechanical Studies of PMMA/PTBF Blends

A. K. KALKAR* and PURNIMA S. PARKHI

Physics Division, Department of Chemical Technology, University of Bombay, Matunga, Bombay 400 019, India

SYNOPSIS

Differential thermal and dynamic mechanical analysis (DTA and DMA) were carried out on the blend system of atactic poly(methyl methacrylate) (PMMA) with poly(*p*-*t*-butyl phenol formaldehyde) (PTBF). In both the techniques, the PMMA/PTBF blend system exhibited a composition-dependent, single glass-transition temperature, indicating miscibility. The blends exhibited composition-dependent morphology dominated by induced cluster formation of PMMA as a separate phase in blends. The DTA scans of blends exhibited broad melting endotherms. Also, in DMA, apart from the main relaxation (tan δ), the system showed an additional high-temperature relaxation (T_u), indicating the presence of a separate phase. In addition, wide-angle X-ray diffraction (WAXD), Fourier-transform infrared (FTIR) spectroscopy, and sonic pulse propagation measurements provide evidence for the formation of PMMA clusters in the bulk PMMA/PTBF blends. The mechanical behavior of the blends is discussed in terms of the variations in shape and magnitude of tan δ, E', and E'' curves. It is concluded that PTBF acts as a compatible plasticizer in PMMA/PTBF blends and, because of changed morphology, improves the elongation of blend films compared to pure PMMA. © 1995 John Wiley & Sons, Inc.

INTRODUCTION

Polymers are seldom used commercially in a pure state as they often require some of their properties to be modified by inclusion of characteristic low-molecular-weight plasticizers. Among the properties of polymers, the mechanical properties are perhaps those of applied importance. In this context, the miscibility and the ratio of these plasticizers in the polymer is crucial and, as a consequence, affect significantly the mechanical properties of the pristine polymer.

Although the novolac resins (an important class of industrial diluents) are widely used as ingredients in paints and adhesives,[1] little work has been reported on their miscibility with high-molecular thermoplastics.[2-6] In fact, the novolacs are ideal blending candidates due to their polar functional groups, which may produce strong interactions[2-6] with other polymers. Such interactions enhance the miscibility. However, the mechanical properties of such polymer diluent blends also depend on the molecular weight of the diluent and the overall resulting polymer–diluent blend morphology.

In continuation of our earlier work[6] on polymer–plasticizer compatibility, in this article we will describe the composition-dependent effects of low-molecular-weight poly(*p*-*t*-butyl phenol formaldehyde PTBF), as an additive, on the miscibility and the mechanical properties of poly(methyl methacrylate) (PMMA).

EXPERIMENTAL

Materials

Medium-molecular-weight atactic PMMA (cat. no. 18224) was obtained from Aldrich Chemical Co. (Milwaukee, WI). The PTBF was synthesized in

* To whom correspondence should be addressed.

Journal of Applied Polymer Science, Vol. 57, 233–243 (1995)
© 1995 John Wiley & Sons, Inc. CCC 0021-8995/95/020233-11

the Plastic Division of this institute by conventional condensation between *p*-*t*-butyl phenol and formaldehyde. It was in an uncurved (linear) solid form. Its molecular weight by vapor pressure osmometry was 1500–1600 ($\overline{DP_n}$ = 10).

Blend Preparation

Blends of PMMA and PTBF in different proportions were prepared by evaporation of 5% w/v of solutions in 1,2-dichloroethane. The samples were dried in vacuum at ambient temperature (30°C) for 5 h. To remove the last traces of solvent, the samples were finally dried under vacuum at 45°C and stored in a dry atmosphere. Thus, the films obtained were transparent and homogeneous. Films with PTBF > 50% in the blends were sticky or brittle. The blend films for infrared spectral studies were prepared separately.

Differential Thermal Analysis (DTA)

DTA was performed with a Stanton–Redcroft simultaneous DTA/thermogravimetric analyzer, Model STA-780. The sample weights were kept constant, and the heating rate was 5°C/min. Prior to analysis, all the blend samples were heated to 150°C and cooled under nitrogen atmosphere in the DTA to provide uniform sample history. For the actual analysis, the first and second runs were obtained for the same loaded sample. The glass-transition temperature, T_g, was taken as the temperature corresponding to the midpoint of the step change in the second DTA scan. The first and second runs gave very similar values (within ±2°C) for the T_gs. The temperature corresponding to the peak maximum from the melting endotherm was taken as the melting point.

Fourier-Transform Infrared (FTIR) Spectral Measurements

FTIR spectra were obtained on a Bruker IFS-88 FTIR spectrophotometer in absorbance mode. The frequency scale with 2 cm^{-1} resolution of spectrophotometer was internally calibrated with a reference helium–neon laser to an accuracy of 0.2 cm^{-1}. The blend films for infrared (IR) spectral measurements were prepared by spreading uniformly a fixed volume of the blend solution on a 1.5-cm-diameter NaCl window. The solvent was allowed to evaporate at room temperature, followed by vacuum drying for 5 h. The final spectra were recorded out of 100 signal-averaged scans. The areas under the characteristic IR bands were calculated using software.

Sonic Velocity Measurements

Sonic velocity (C) measurements were made on a Dynamic Modulus Tester, Model PPM-SR (H. M. Morgan Co., Inc., Norwood, MA) at frequency 5 kHz and at room temperature. The sample in the form of a long strip with uniform thickness was used. Multisets of readings were taken on different places of the sample. The average of these values of C was used for the calculations of the modulus of elasticity (E) using the relation $E = ep^2$, where p is the density (g/cc) of the sample.[7] The densities of the films were measured by Moore and Sheldon's flotation technique.[8] In the present case, a mixture of butan-1-ol (AR grade) with a density of 0.810 g/cc and carbon tetrachloride (AR grade) with a density of 1.592 g/cc was used. These measurements were possible containing up to a maximum of 70 wt % of PTBF in the blends.

Wide-Angle X-Ray Diffraction (WAXD)

X-ray diffraction patterns of the blend films and PMMA (90×10^{-6} m thick) were recorded employing a Philips model-1710 X-ray diffractometer fitted with the Cu-K_α radiation source. The intensity versus Bragg angle (2θ) scan data were collected in a symmetrical reflection mode at 0.2° intervals for the angular range from 2 to 36° (2θ) with a scanning rate 2°/min. The WAXD spectrum of PTBF was recorded by mounting PTBF as a highly pressed thin pellet. A similar procedure was also used for the blends with ≥ 80 wt % of PTBF. The samples were of the same thickness, and the same area was exposed, which corresponds to sample holder window dimensions 1.5 cm × 1.0 cm.

Dynamic Mechanical Analysis (DMA)

DMA measurements were obtained by using a direct reading Rheovibron DDV-II C, Rheo-200 dynamic tensile tester (Toyo Measuring Instruments, Ltd., Japan). For every experiment, the sample was a piece of size 0.5 × 2 cm^2 and was held tightly between the chucks in a temperature-controlled high-temperature chamber. The data were measured at 35 Hz from 20° to 90°C, using a heating rate of 2°C/min. The measurements were restricted to blends up to 50/50 composition because no suitable blend films for firm grip between the chucks could be formed with > 50 wt % of PTBF. The mechanical

loss factor, tan δ, and dynamic module (E', E'') were observed.

Tensile Strength Measurements

Tensile strength and elongation were measured on an Instron tensile tester. A film of 1 cm was gripped between two jaws such that the specimen length was about 3 cm and the breaks occurred in the machine direction of the film. The speed of the head was 50 mm/min. The average breaking load and elongation at break were calculated from a set of 15 measurements. Using these data, the Young's modulus for the films was calculated. The measurements were restricted to the blends up to 50 wt % of PTBF due to the lack of a firm grip of films with $\geq$ 60 wt % of PTBF.

RESULTS AND DISCUSSION

Thermal Analysis (DTA)

DTA studies were performed on PMMA, PTBF, and PMMA/PTBF blends. Neat PMMA and PTBF exhibited T_gs at 105°C and 51°C, respectively, and showed no evidence of crystallization. The DTA thermograms of PMMA/PTBF blends are shown in Figure 1, and the T_g versus PTBF content in the blends is plotted in Figure 2 as triangles. In each thermogram of blends, two thermal transitions are observed.

The lower temperature transition behaves as the composition-dependent T_g of bulk PMMA/PTBF blends, whereas the higher temperature transition is due to a typical composition-dependent induced morphological change, and is a melting endotherm (T_m).

The thermal studies show clearly that the PMMA/PTBF blend system exhibits a single composition-dependent T_g over an entire range of compositions. This implies that the bulk blend system is miscible. The apparent miscibility is due to the specific intermolecular interaction (— C=O · · · H — O —) between the carbonyl group of PMMA and the hydroxyl group of PTBF.

The T_g versus blend composition curve, however, does not have a universal simple relationship with Fox's equation[9] curve but has variations, reflecting the complex morphology of the blend system (Fig. 2). Large negative deviations of the experimentally observed T_g from the calculated weight average values were observed. The unusual behavior of the T_gs is attributed to a creation of a free volume due to a

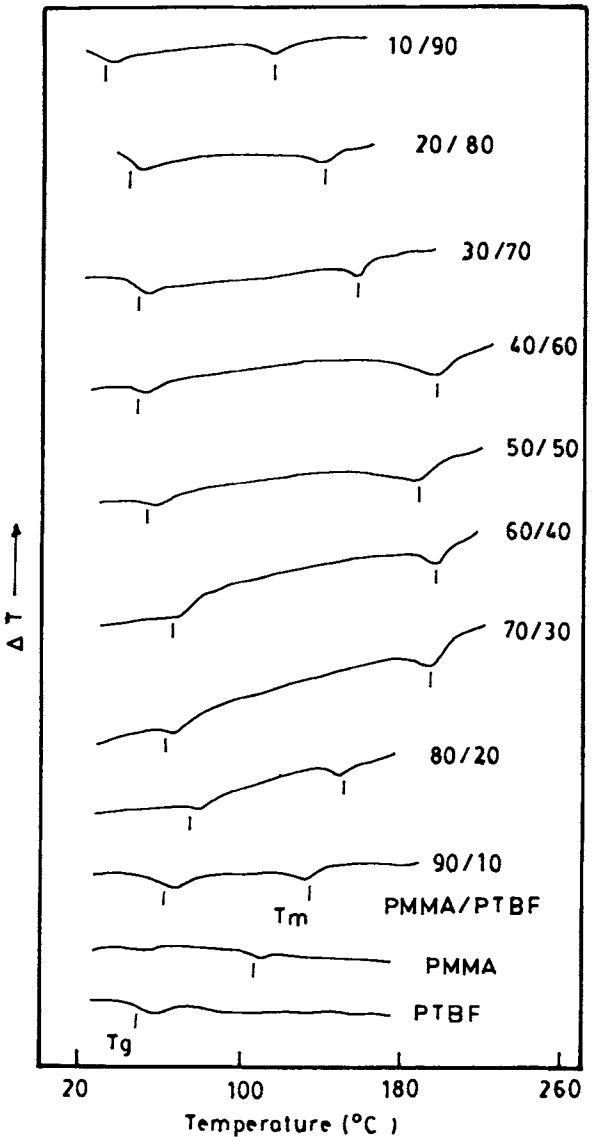

Figure 1 Composition-dependent DTA thermograms illustrating T_g and T_m for PMMA, PTBF, and PMMA/PTBF blends.

manifested plasticizing effect in the blend system with low PTBF content (< 50 wt %). However, for the blends with higher wt % of PTBF (> 50 wt %), the hydrogen bonding effect, along with the plasticizing effect, also contributes to enhancing the glass-transition temperature. The increase in free volume can be understood in terms of the interchain interactions in the blend system. The additive molecules (in the present case, PTBF) align themselves either along the backbone chain or along the side groups (of PMMA). When a long additive molecule like PTBF aligns itself along a side group (the size of the side group being smaller than the additive mol-

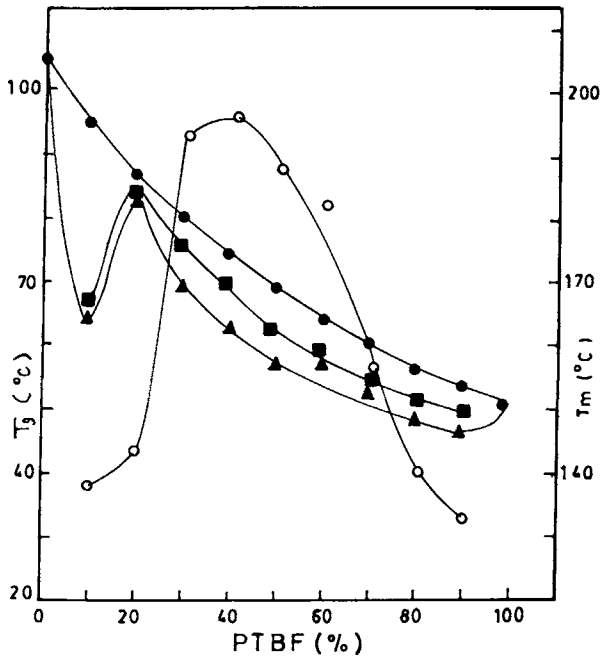

Figure 2 Composition dependence of the T_g and T_m of PMMA/PTBF blends: (▲) DTA; (●) Fox equation; (■) Gordon–Taylor equation; (○) T_m.

ecule), the chains are pushed apart from each other. As a result, interchain interaction will decrease, free volume will increase, and sidechain motion only will be affected. Hence for the backbone chain, the additive will work as a diluent, resulting in shift of T_gs to extra lower temperatures in blends.

With increasing PTBF content in blends, the competitive specific hydrogen bond interaction dominates the plasticizing effect and thus restricts the backbone chain motion. Thus, now the observed T_gs of blends comparatively shift toward higher temperatures. However, they still exhibit a large negative deviation with respect to calculated values (Fig. 2). Furthermore, the modified Gordon–Taylor equation,[10] with the quadratic term $q\ W_1W_2$ representing the contribution due to hydrogen bonding to effective crosslinks, was found to give unsatisfactory agreement with observed T_g behavior even for the best-fit parameters values of $K = 0.57$ ($K \neq 1$) and $9 = 22.87$ ($q \neq 0$). These values were obtained by using the logarithmic form of the Gordon–Taylor equation.[11] The best-fit T_g curve is shown in Figure 2.

The DTA thermograms of blends exhibit another composition-dependent transition temperature (Fig. 2) in the 130–190°C temperature range. The repeated thermograms, obtained using thick sample films (90×10^{-6} m thick), clearly indicate the endothermic nature of the transition. It is observed that for the low content of PTBF (≤ 40 wt %) in the blends, the transition temperature gradually increases and reaches to 197°C for 60/40 composition. However, with a further increase in the PTBF content (≥ 50 wt %), the temperature decreases and is 132°C for 10/90 PMMA/PTBF composition. However, the PMMA used in the present case is atactic and does not crystallize but aggregates.[12–18] In ac-

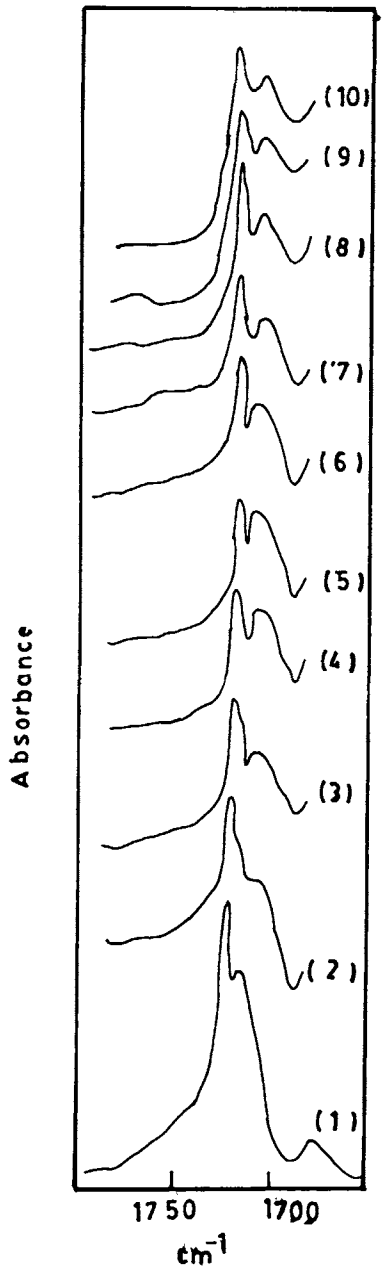

Figure 3 FTIR spectra in the carbonyl region of PMMA (1) and PMMA/PTBF blends: (2) 90/10; (3) 80/20; (4) 70/30; (5) 60/40; (6) 50/50; (7) 40/60; (8) 30/70; (9) 20/80; and (10) 10/90.

cordance with a considerably high value of transition, this indicates the melting of the separated noncrystalline aggregate domains[15-17] rather than a second glass-transition temperature corresponding to a separate PMMA matrix/PTBF phase due to a possible hydrogen-bond-induced macrosynergetic effect. The WAXD and FTIR evidence, discussed later in this article, supports this conclusion. The induced new structure domains are of a denser packing of the PMMA molecules, but with new, more preferred and ordered arrangement than the original PMMA. This type of aggregation is called clustering, and these clusters do not crystallize in absence of three-dimensional packing.

It seems that the dominant plasticizing effect of PTBF and subsequently the hydrogen bonding modifies the shear forces in the blends, which orients the rigid helical structures in some of the PMMA chains. This ultimately leads to growth of PMMA clusters in the blends. The formation of such a noncrystalline aggregates imbalances the wt % of PMMA in blends, which ultimately also contributes to deviation in observed and calculated T_gs of blends.

Fourier-Transform Infrared Spectral Analysis

It is well established that the frequencies associated with the preferred conformations are distinct from those associated with amorphous conformations.[18] In the present case, to explore the contribution due to composition-dependent induced preferred conformations in the PMMA [due to hydrogen bond formation (—C=O···H—O—) between the two components] in PMMA/PTBF blends, we have followed the changes in the carbonyl stretching frequency region.

Figure 3 shows the spectra in the region from 1700 cm^{-1} to 1800 cm^{-1} of these blends along with those of pure PMMA. The carbonyl stretching vibration of PMMA occurs at 1741 cm^{-1}. The appearance of a new bond at 1718 cm^{-1} in blends which exhibit the composition-dependent intensity variation is attributed to preferred conformations, representing the induced PMMA clusters. Figure 4 illustrates the areas of the peaks under 1718 cm^{-1} bands as a function of the PTBF content in the blends. Considering the area under the 1718 cm^{-1} band proportional to the formation order of the PMMA clusters in the blends, it is observed that initially this area is increasing with an increase in PTBF content. However, later, for blends with ≥ 50 wt % of PTBF, this area gradually decreases.

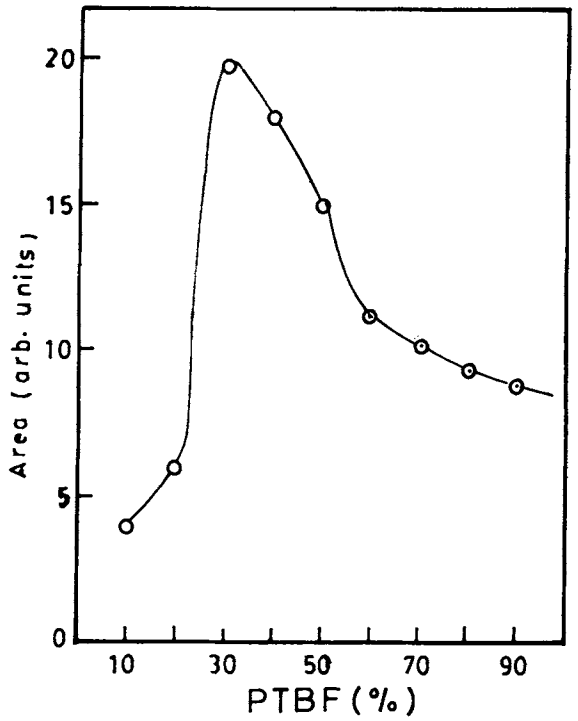

Figure 4 Plot of area under the 1718 cm^{-1} infrared absorption band (carbonyl stretching band—preferred conformation in PMMA) versus percent PTBF in PMMA/PTBF blends.

Sonic Velocity Measurements

Sonic pulse velocity measurements reveal various aspects of the morphological changes at the molecular level.[19-21] The results of acoustic measurements for the PMMA/PTBF are depicted in Figure 5. Inspection of the results shows that the initially sonic velocity (C) decreases for 90/10 and 80/20 blend composition in comparison to pure PMMA and then increases with increasing PTBF content in the blends. A similar trend has been observed in case of sonic modulus (E). Such behavior clearly indicates the active plasticizing action of PTBF for PMMA. However, the increase in the magnitudes of C and E after an inversion region with increasing PTBF content in blends is ultimately attributed to the enhanced intermolecular interaction, which, in turn, results in greater rigidity of the main chains of PMMA. This tends to stabilize more ordered arrangement of PMMA chains, facilitated via hydrogen bond interactions, which ultimately results in induced anticrystalline clusters of PMMA in the blends. The higher magnitude of E and C for 70/30 composition is due to enhanced energy of intermolecular interaction between the PMMA and PTBF rather than in adjacent PMMA chains. Such a mor-

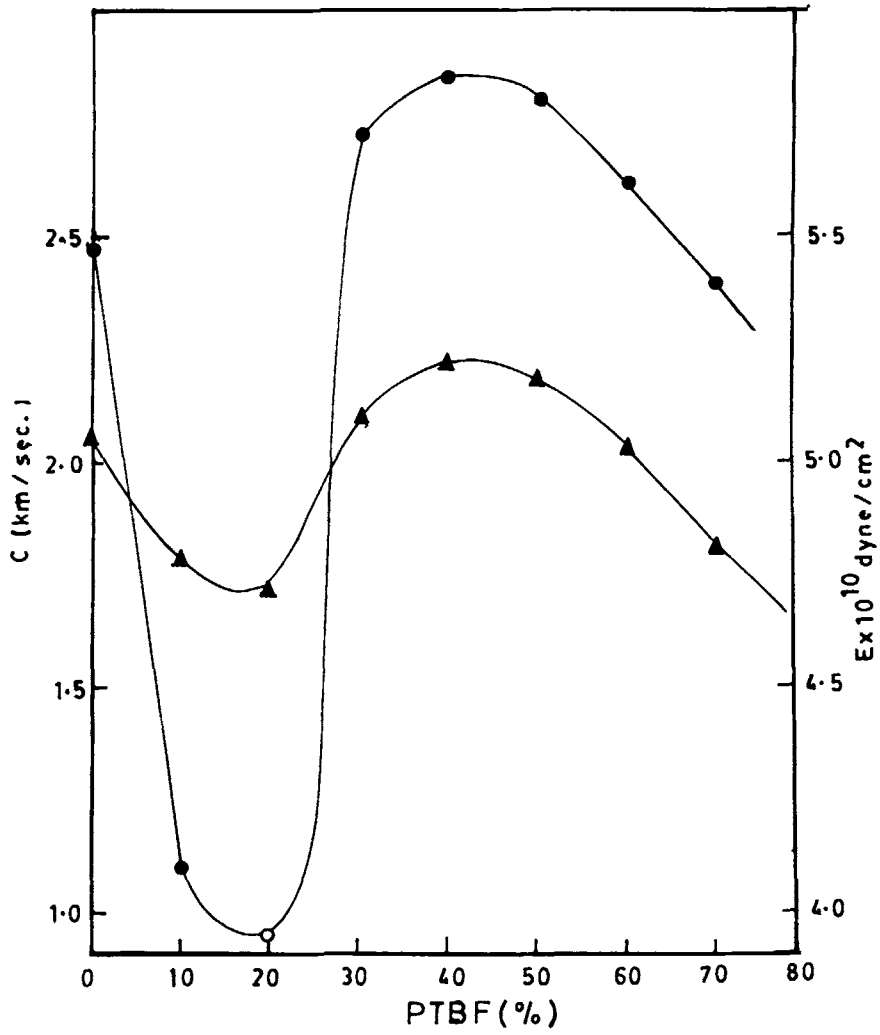

Figure 5 Variation in sonic velocity (●) and sonic modulus (▲) in PMMA/PTBF blends.

phological situation shifts the T_m transition temperature (in DTA) toward higher temperatures for the blend compositions with ≥ 50 wt % of PTBF due to gradual increase in the PMMA chain packing in clusters.

X-Ray Diffraction Analysis

WAXD is the preferred technique for determining morphological structural changes in polymers. The aggregation behavior of atactic PMMA (a-PMMA) is well documented.[22-24] The WAXD from a-PMMA is very similar to that of (s-PMMA).[23] Figure 6 shows the X-ray scattering for the a-PMMA and PTBF samples used in the present studies (curves 2 and 1, respectively).

The broad dominating haloes at 14° and 18° (2 θ) in PMMA and PTBF, respectively, clearly indicate that both the samples are predominantly in an amorphous state. As can be seen upon blending PTBF, the WAXD profile differs greatly from control a-PMMA and develops sharp haloes at 28.7° and 9.4° (2 θ), indicating morphology changes in blends. Further, it is observed that the intensity of these haloes increases up to ≤ 50 wt % of PTBF with decreasing half-peak width. However, with ≥ 60 wt % of PTBF in the blends, the intensity of the haloes decreases, but without changes in the half-peak width. It is observed particularly that with increasing PTBF content in the blends, the halo at 14° (2 θ) sharpens and exhibits splitting, with two peaks at 14.5° and 13.3° (2 θ). This may be due to induced preferential trans-conformation with regular sequences of an average length of 16–20 backbone bonds in a-PMMA,[23] which consequently ends with the formation of a noncrystalline local order of associated PMMA chain segments. This may be due to the absence of a three-dimen-

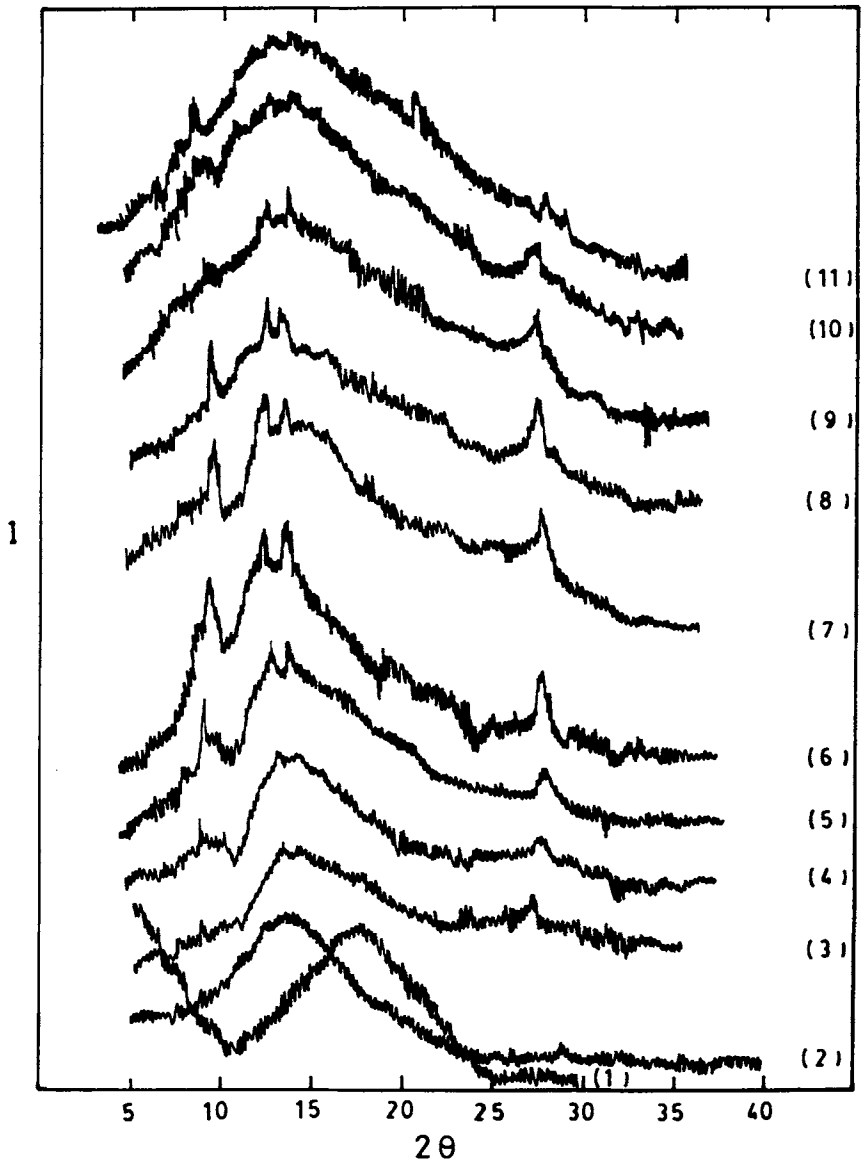

Figure 6 WAXD spectra of PMMA/PTBF blends.: Curve 1: PTBF; 2: PMMA; 3: 90/10; 4: 80/20; 5: 70/30; 6: 60/40; 7: 50/50; 8: 40/60; 9: 30/70; 10: 20/80; 11: 10/90 PMMA/PTBF.

sional crystalline packing of the crystalline subunits of double helices.

Dynamic Mechanical Analysis

In contrast to DTA results, the DMA thermograms exhibit detailed morphological behavior over a wide range of temperatures, indicating the different nature of response of the molecular segmental motions. An attempt has been made to analyze the dynamic mechanical behavior in terms of variation in tan δ, storage modulus (E'), and loss modulus (E'') of this blend system along with PMMA. The dynamic mechanical spectra were measured at 35 Hz, ranging from +20°C to +100°C.

Many investigations have been made of the viscoelastic properties of PMMA.[25-27] The results of measurements made by us in a-PMMA are reproduced in Figure 7(a). The four peaks are observed on the plot of tan δ—namely, at 84°, 72°, 41°, and 28°C. The temperature transition at 84°C corresponds to the temperature at which the segmental mobility of PMMA is unfrozen. This is the highest temperature transition (α-transition) and is assigned as a T_g, which marks the limit of long-range motions of chain segments.

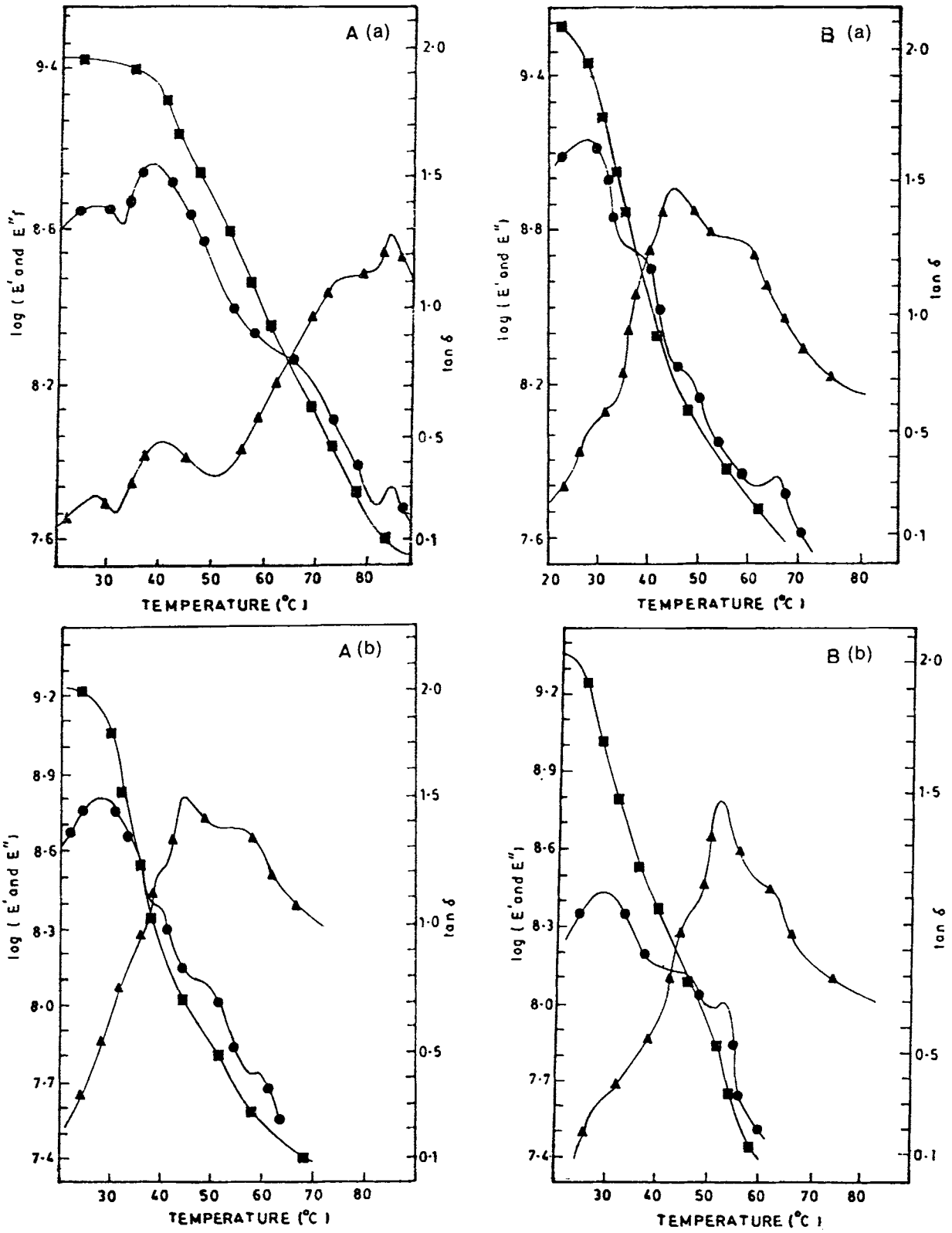

Figure 7 (a) Dynamic mechanical spectra—(▲) tan δ; (●) E'; (■) E''—at 35 Hz of the PMMA/PTBF blends with compositions (A) 100/0 and (B) 90/10. (b) Dynamic mechanical spectra—(▲) tan δ; (●) E'; (■) E''—at 35 Hz of the PMMA/PTBF blends with compositions (A) 80/20 and (B) 70/30. (c) Dynamic mechanical spectra—(▲) tan δ; (●) E'; (■) E''—at 35 Hz of the PMMA/PTBF blends with compositions (A) 60/40 and (B) 50/50.

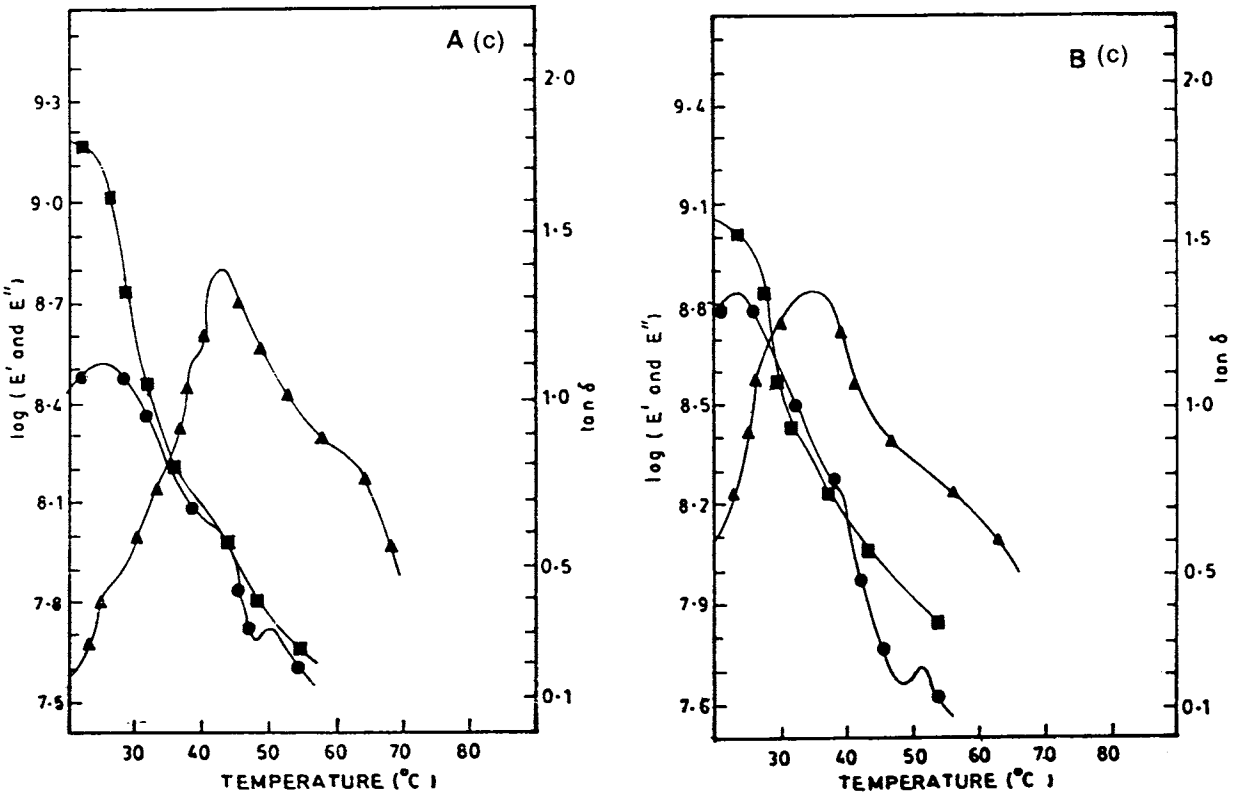

Figure 7 (*Continued from the previous page.*)

The β-transition, observed as one broad β-relaxation maximum, has a multiplet nature. Two temperature transitions at 75° and 41°C have been clearly observed. The various possible origins of the β-transition have been discussed in the literature. It is assumed that β-transition is due to the rotation of the backbone chain relative to the longitudinal axes of PMMA, including the retarded rotation made of the methoxy carbonyl groups in the sidechain. This explains well the creep of PMMA. However, it is also reported that the β-transition basically originates due to the hindered rotation of the ester group about the C—C bonds that links it to the backbone.[28] We prefer the latter assignments. Accordingly, the temperature transition at 41°C is due to the motion of the sidechains of the ester group, whereas the transition at a higher temperature (72°C) may be due to rotation of methoxy carbonyl groups in the sidechain. The temperature transition at 28°C has been assigned as γ-transition and is associated with the motions of the methyl groups attached to the side branches. Thus, these low-temperature β-transitions essentially exhibit relaxation processes due to the motion of the side groups or small elements of the backbone chain. Also, the β-relaxation in PMMA is understood to be the process connected with reorientation motion of the sidechains.[29] No such dynamic mechanical spectrum could be recorded for pure PTBF due to the uncured state, resulting in non-film-forming properties and extreme brittleness.

The dynamic mechanical spectra for 90/10, 80/20, 70/30, 60/40, and 50/50 blend compositions were obtained. As mentioned earlier, no proper films could be formed for the blend compositions with more than the 60 wt % of the PTBF. Figures 7(a), 7(b), and 7(c) show the dynamic mechanical properties in terms of variation in internal friction or mechanical damping (tan δ), dynamic storage modulus (E'), and loss modulus (E'').

It is interesting to note that dynamic modulus curves (E') of blends have an early inflection point. This is the region where the β-transition peak goes through a maximum. Thus the dispersion starts to occur in the secondary transition region (glassy state) rather than the soft rubbery state (glass-transition region). The curves (E'), however, also exhibit a second low-magnitude inflection point, of which the tan δ curves (at T_g) have the maximum. Accordingly, the loss modulus (E'') curves go through a peak maximum corresponding to β-transition. It seems that the maximum heat dissipation per unit

deformation initiates in the secondary transition region.

The shape and closeness of the various transitions observed on mechanical loss factor (tan δ) and dynamic loss modulus (E'') curves are characteristic dynamic mechanical features in the present blend system. The pendent group in PMMA has a significant length, and hence the relaxation is somewhat a combined α, β-process. In such cases, the segmental motion is coupled with side group motions. However, in the present blend system the intensity of the β-relaxation peak goes on decreasing with increasing PTBF content in the blends for 90/10, 80/20, and 70/30 compositions. This indicates the increasing interaction, which again hinders the side group of segmental motion, thus shifting the α-relaxation (maximum tan δ) to higher temperatures. However, for the increase of PTBF content in the blends for 60/40 and 50/50 compositions, the intensity of the β-peak again increases, but with the peak broadening toward higher temperature. This may be attributed to the changed morphology in the blends, as mentioned earlier, due to the noncrystalline PMMA cluster domain formation in the blends.

Of greatest interest is the double temperature transition in the main relaxation (in tan δ curves) region of the blends. As mentioned earlier, the higher temperature transition in DMA with respect to the glass-transition temperature in the blends can be understood in terms of the presence of a cluster structure in a-PMMA. No such higher temperature transition could be located for neat a-PMMA in our experiments. Thus, this cannot be a solvent-induced morphology change in blends but is due to the PTBF-induced changes.

The high-temperature transition mentioned earlier is generally designated as the T_{ll} (α') relaxation and involves a premelting process. In the present case, it occurs at 56°C for 90/10 composition and increases to 60°C for 60/40 composition. It seems that the induced PMMA cluster in blends initiates as nucleation in 90/10 and grows with increasing PTBF content in blends. However, for blend composition 50/50, it reduces to 57°C. This may be attributed to the bulky, loose optimum geometry of the PMMA clusters.

Mechanical Properties

It will be interesting to note the effect of the formation of the noncrystalline aggregate PMMA domains in blends on overall mechanical properties of the blends. The magnitudes of the maxama in the E' and E'' curves of the blends in comparison to pure the PMMA curve are the indicative parameters in the present case. The overall E' magnitudes of blends (say at 22°C) in the glassy-state region exhibit slight enhancement over pure PMMA. This indicates very marginal improvement in the mechanical properties of blends.

The variation in tensile strength and elongation of these blends is illustrated in Figure 8 and supports this conclusion. It is observed that as the content of PTBF to PMMA increases, the breaking strength of the films decreases compared to that of pure PMMA while the elongation of pure PMMA film is less than that of the films of blends. This is due to the changed morphology in blends, which influences the segmental motions in the amorphous phase.[30] However, in the present case the height of loss peaks (at transition) in blends is always greater than the unity. This indicates the amorphous bulk nature of the blends.[31]

CONCLUSION

The PMMA/PTBF blend system is miscible in the larger amorphous phase at all compositions but forms good films only up to 50/50 compositions.

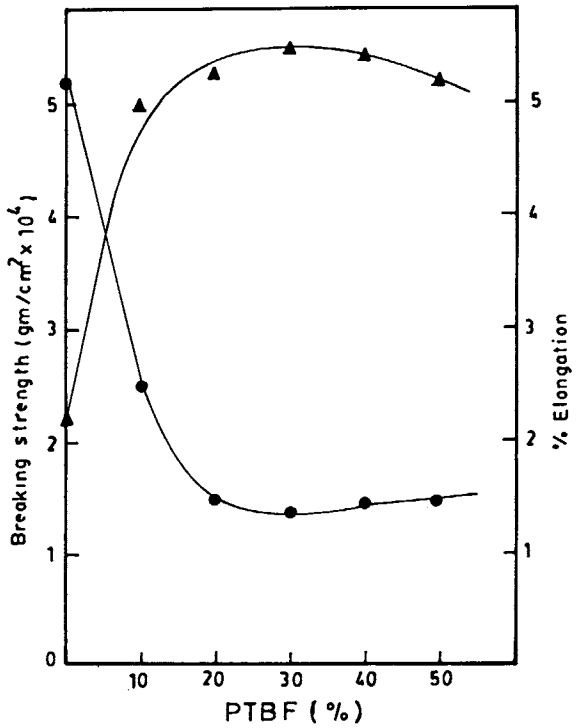

Figure 8 Tensile strength (●) and the percent elongation (▲) of the PMMA/PTBF blends.

Overall, the PTBF acts as a compitable plasticizer. However, the blend system clearly exhibits a composition-dependent melting endotherm in DTA attributed to phase-separated PMMA clusters in the blends. The composition-dependent high-temperature transition ($T_{ll} > T_g$) in DMA and WAXD, FTIR, and sonic pulse propogation studies indicates the changed morphology in terms of PMMA clustering in bulk PMMA/PTBF blend material. It is observed that this influences the mechanical properties of blend films. The blend films have improved elongation compared to PMMA, with an optical clarity similar to that of PMMA.

We thank Professor M. M. Sharma, Director, Department of Chemical Technology, for the use of the FTIR spectrophotometer (under the Committee on Infrastructure in Science and Technology (COSIST) program). We are also grateful to Dr. M. A. Shenoy of the University of Bombay Department of Chemical Technology for the PTBF sample.

REFERENCES

1. A. Knop and W. Scheib, *Chemistry and Application of Phenolic Resins,* Springer-Verlag, New York, 1979.
2. J. R. Pennacchia, E. M. Pearce, T. K. Kwei, B. J. Bulkin, and Jong-Pyng Chen, *Macromolecules,* **19,** 973 (1983).
3. P. Lin, C. Clash, E. M. Pearce, and T. K. Kwei, *J. Polym. Sci. Polym. Phys. Ed.,* **26,** 603 (1988).
4. T. K. Kwei, *J. Polym. Sci. Polym. Lett. Ed.,* **22,** 307 (1984).
5. S. R. Faherenholtz and T. K. Kwei, *Macromolecules,* **14,** 1076 (1981).
6. A. K. Kalkar and N. K. Roy, *Eur. Polym. J.* **29,** 1391 (1993).
7. W. W. Moseley, Jr., *J. Appl. Polym. Sci.,* **3,** 266 (1960).
8. W. R. Moore and R. P. Sheldon, *Polymer,* **2,** 315 (1961).
9. T. G. Fox, *Bull. Am. Phys. Soc.,* **2,** 123 (1956).
10. M. Gordon and J. S. Taylor, *J. Appl. Chem.,* **2,** 493 (1953).
11. M. A. DeAranjo, R. Stadler, and H. J. Cantow, *Polymer,* **29,** 2235 (1988).
12. L. Mrkvickova, J. Stejskal, J. Spevacek, J. Horska, and O. Quadrat, *Polymer,* **24,** 700 (1983).
13. W. Borchard, M. Pyrlik, and G. Rehage, *Makromol. Chem.,* **145,** 169 (1971).
14. W. Borchard, G. Kalawritinos, B. Mohadjer, M. Pyrlik, and G. Rehage, *Angew. Makromol. Chem.,***29/30,** 471 (1973).
15. R. H. G. Brinkhuis and A. J. Schouten, *Macromolecules,* **24,** 1496 (1991).
16. A. De Boer, G. O. R. Alberda van Ekenstein, and G. Challa, *Polymer,* **16,** 930 (1975).
17. K. Konnecke and G. Rehage, *Colloid Polym. Sci.,* **259,** 1062 (1981).
18. M. M. Colemann and P. C. Painter, *Appl. Spectrosc. Rev.,* **20,** 255 (1984).
19. R. Suresh, Y. P. Sing, G. D. Nigam, and R. P. Singh, *Eur. Polym. J.,* **20,** 739 (1984).
20. B. Hartmann, *Acoustic Properties,* in *Encyclopedia Polym. Sci. Eng.,* Vol. 1, p. 131, 2nd ed., Wiley, New York, 1985.
21. Y. P. Sing and R. P. Singh, *Eur. Polym. J.* **19,** 529 (1983).
22. M. Pick, R. Lovell, and A. H. Windle, *Polymer,* **21,** 1017 (1989).
23. R. Lovell and A. H. Windle, *Polymer,* **22,** 175 (1981).
24. G. R. Mitchell and A. H. Windle, *Polymer,* **24,** 285 (1983).
25. S. G. Turley and H. Keskkula, *J. Polym. Sci.,* **C14,** 69 (1965).
26. J. A. Roetling, *Polymer,* **6,** 311 (1965).
27. R. F. Boyer, *Polym. Eng. Sci.,* **8,** 161 (1968).
28. C. J. T. Landry and P. Mark Henriches, *Macromolecules,* **22,** 2157 (1989).
29. J. A. Sauer and R. G. Saba, *J. Macromol. Sci.,* **A3-7,** 1217 (1969).
30. K. H. Illers and H. Breuer, *J. Colloid. Sci.,* **18,** 1 (1963).
31. J. V. Koleske and R. D. Lundberg, *J. Polym. Sci. Polym. Phys. Ed.,* **7,** 795 (1969).

Received September 6, 1994
Accepted January 10, 1995